Chapter 5

The Effects of Flue-gas Recirculation on Fenimore NO Formation in Low-Pressure, Fuel-Rich Premixed $CH_4/O_2/N_2$ Flames

5.1 Introduction

Flue gas recirculation (FGR) is one of the oldest and most widely used techniques for reducing NO_x emissions in industrial natural gas-fired combustion equipment [1]. In this Chapter we focus our attention to so-called 'dry' FGR, which indicates that water is removed from the flue gases. This is often done in practice, to prevent condensation of water, and concomitant corrosion, in the piping bringing the flue gases from the exhaust to the burner. The effect of FGR on fuel-lean and stoichiometric flames is quite well known, where, as discussed in Chapter 1, the reduction in temperature strongly decreases NO formation via the Zeldovich mechanism. However, the effect in fuel-rich flames, where the Fenimore mechanism is the major route to NO formation, is relatively unknown.

Mokhov and Levinsky [2] studied the effectiveness of burner stabilization (see also Chapters 1 and 4) and FGR in laminar atmospheric pressure stoichiometric and fuel-rich (ϕ=1.3) premixed methane/air flames. For the stoichiometric flame, when plotted as a function of flame temperature, the effect of burner stabilization and FGR on the measured NO mole fraction were seen to be identical. However, for the fuel-rich flame, the measured NO mole fractions for FGR are significantly higher than those in flames with upstream heat loss at the same flame temperature. When comparing the experimental results with calculations based on the GRI-Mech 3.0 chemical mechanism [3], the predicted NO mole fractions are in good quantitative and qualitative agreement for the stoichiometric flame, but the calculations substantially overpredicted the NO mole fractions of the fuel-rich flame.

To obtain insight into the changes in flame structure responsible for the influence of FGR on NO formation, it would be interesting to examine these effects in low-pressure premixed flames, where the quantitative determination of the profiles of key intermediates such as the CH radical are possible. Although a number of studies have provided insight into the Fenimore mechanism in low-pressure flames [4-7], to our knowledge, the effect of FGR on low-pressure flames has not been studied previously. In this Chapter, we investigate the effects of FGR on Fenimore NO formation in 35 Torr ϕ=1.3 premixed methane/oxygen/nitrogen flames by measuring the profiles of temperature, OH, CH and NO using laser-induced fluorescence (Chapter 3).

Since the effects of burner stabilization for this flame have been discussed in Chapter 4, we will compare the results reported there with those obtained using FGR, in order to compare the effectiveness of the two NO_x control strategies under fuel-rich conditions.

5.2 Experimental details

The degree of recirculation $\gamma = \alpha + \beta$ [see equation (2.1)] is chosen based a series of calculations, using the PREMIX code [8] and GRI-Mech 3.0. The starting point of the calculations are the results presented in Chapter 4, where the influence of burner stabilization on Fenimore NO formation in 35 Torr fuel-rich (ϕ=1.3-1.5) premixed methane/oxygen/nitrogen flames with flow rates of 3, 4 and 5 slpm was studied. The criterion is to find a stable flame with FGR having a maximum temperature close to that of a flame without FGR at 3 slpm. Unfortunately, flames without FGR at ϕ>1.3 are on the edge of instability (close to the free flame burning velocity), and become unstable when applying FGR. For this reason, we have chosen the flames described previously at 35 Torr and ϕ=1.3. An additional benefit of using this flame is that CHEMKIN calculations show excellent agreement with measured temperature and OH, CH and NO mole fractions (Chapter 4).

The calculations indicate that a slightly stabilized flame with a flow rate of 4 slpm at γ=3 satisfies the criterion. To estimate a possible additional influence of stabilization, the measurements are performed also in the free flame with the same value of γ. The experimental conditions for flames without FGR (Flames B, as in Chapter 4) and with FGR (Flames F) are summarized in Table 5.1:

Flame[a]	γ	Flow rate[b] (slpm)	$T_{max}exp$ (K)	$X_{CH}exp$ (ppm)	$X_{NO,1.5}\,exp$[c] (ppm)	$X_{NO}\,calc$[c] (ppm)	$X_{NO,Fen}$ (ppm)
B1	0	3	1935	18.8	33.0 ± 5.0	37.8	34.1
B2	0	4	2090	24.5	40.9 ± 6.1	44.2	45.3
B3	0	5	2200	35.4	50.6 ± 7.6	53.6	50.1
F2	3	4	1947	14.2	33.4 ± 5.0	34.7	41.3
F3	3	4.8[d]	1997	14.3	37.1 ± 5.6	38.3	38.7

[a]Flames without FGR are indicated with "B"(see also Chapter 4), whereas flames with FGR are indicated with "F". In both cases: p = 35 Torr and $[O_2]/[N_2]+[O_2]=0.4$ [b]1 slpm corresponds to ~0.0007 g/cm^{2}s [C] At axial distance of 1.5 cm [d] free flame velocity

Table 5. 1: Flame conditions and data for CH and NO measurements and Analysis (see text for details)

The experimental setup described in Chapter 2 is used for performing the experiments. Flame temperature and absolute OH, CH and NO mole fractions are determined using LIF following the procedure described in Chapter 3. As described there, the temperature is determined using integrated area of 10 rotational states of the $A^2\Sigma^+$-$X^2\Pi$ (0,0) band of OH radical in a Boltzmann plot, with an estimated uncertainty of ±50-75 K. The measured temperature profiles are approximated by equation (3.19) and used as input for the CHEMKIN calculations for Flame F2, while the energy equation is solved for Flame F3. The estimated accuracy of the OH, CH and NO mole fractions is better than 20%, 25% and 15%, respectively. The experimental results presented here are an average of several measurements: for each species the measurements are reproducible within 10 %.

5.3 Temperature and OH profiles

The measured temperature and OH mole fractions in the 35 Torr ϕ=1.3 premixed methane/oxygen/nitrogen flames with FGR are shown in Figure 5.1 (F2 and F3). For comparison, experimental results received in flames with the same mass flux but without FGR (B2 and B3) are shown in Figure 5.1 as well. As can be seen, changing composition of unburned fuel/oxidizer mixture by adding flue gases results in substantial decrease in flame temperature (~200 K) and OH concentration (~ 30%). Based on earlier observations [2,9,10] on

atmospheric pressure flames, we expect that this decrease in maximum temperature and OH mole fraction as a consequence of FGR will be reflected in the NO mole fractions as well, which will be discussed below.

It is interesting to point out that the OH and temperature profiles for flames with FGR (F2 and F3) are shifted away from the burner surface in comparison with flames without FGR (B2 and B3). As result of this 'shift', the properties of the flames F2 and F3 are very similar and close to those of adiabatic free flames. Figure 5.1 also shows calculated OH mole fractions obtained from CHEMKIN calculations based on measured temperature profile, except for Flame F3 that is calculated as a free flame (see above). As seen in Chapter 4, the calculated OH mole fractions are very sensitive to the temperature profiles; thus the excellent agreement between measured and calculated OH profiles for most of the measured domain gives us confidence in the temperature determination.

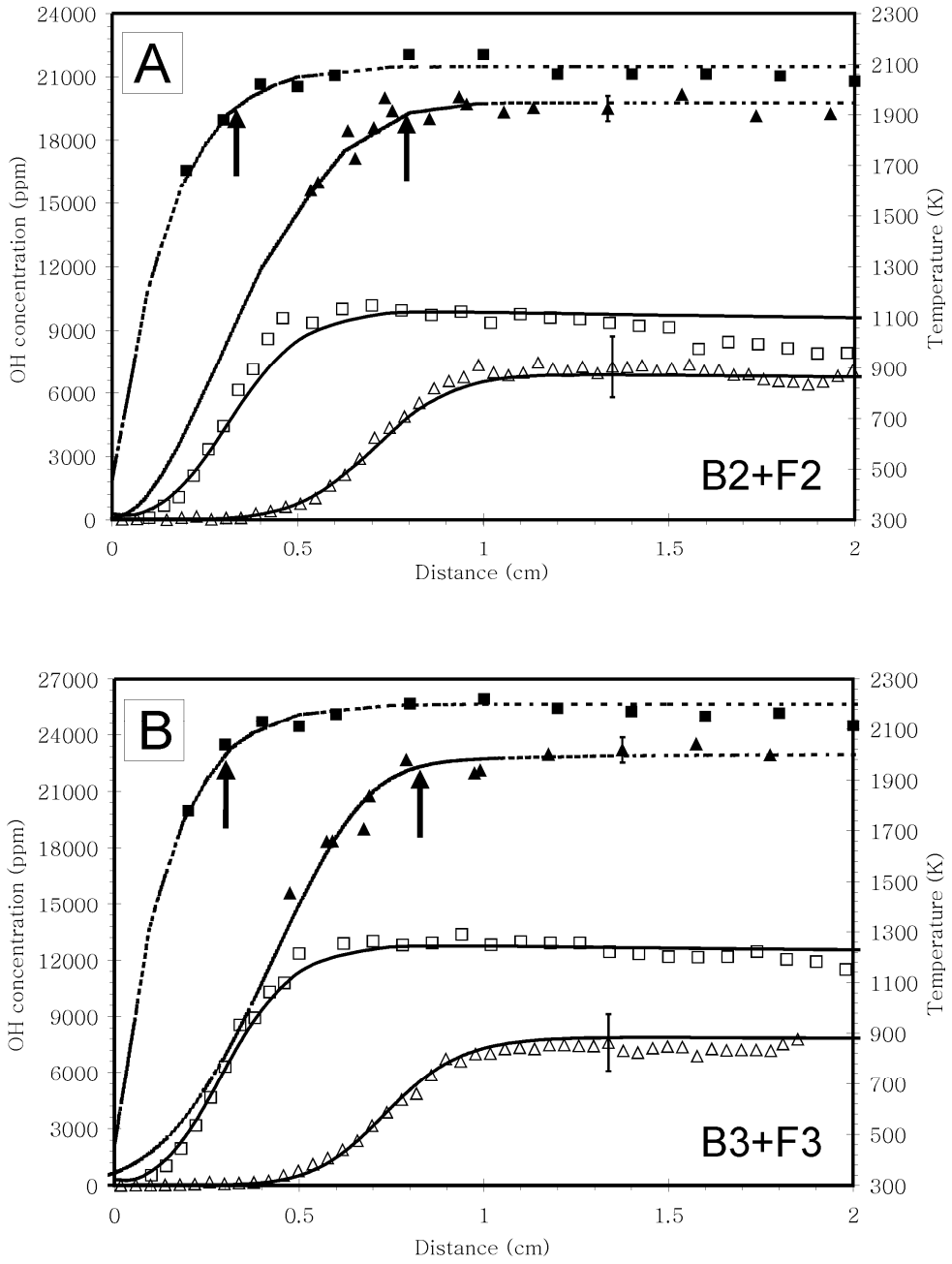

Figure 5. 1 Measured and calculated OH and temperature profiles for

A) Flames B2 (4 slpm without FGR) and F2 (4 slpm with FGR)

B) Flames B3 (5 slpm without FGR) and F3 (4.8 slpm with FGR).

Points denote measurements: squares for flame B2(5.1A) and B3 (5.1B), triangles for Flame F2(5.1A) and F3(5.1B). Open symbols are OH profiles and filled symbols are temperature profiles. Lines denote calculated results: dashed lines are temperature and solid lines are OH. Arrows indicate the position of maximum CH concentration for both flames.

5.4 CH and NO profiles

The measured and calculated profiles of the CH and NO mole fractions in Flames F2 and F3 are shown in Figure 5.2. Both the maximum measured CH mole fraction ($X_{CH\ exp}$) and the measured NO mole fraction at 1.5 cm ($X_{NO,1.5}$) are presented in Table 5.1. To facilitate the analyses, the predicted CH and NO profiles obtained from the CHEMKIN calculations are shown as well. The measured and predicted NO profiles show good agreement. The maximum CH concentration and the width of the CH profiles also correspond very well with predictions.

As can be seen from Figure 5.2, measured CH profiles are shifted (~0.1 cm) away from the burner surface compared to the predictions. Although experimental error cannot be excluded, the observed shift can also be the result of an incorrect prediction of the CH profiles. Since the calculations predict the NO concentrations quantitatively, the question arises as to the consequences of this shift for the analysis of the NO measurements. To assist the assessment of this shift, it will be helpful to estimate the amount of NO produced via the Fenimore mechanism ($X_{NO,Fen}$) using equation (1.11) and the measured CH and temperature profiles, as was done in Chapter 4. The integration is performed up to 1.5 cm above the burner surface and the results are presented in Table 5.1. As discussed in Chapter 4, we estimate the values of $X_{NO,Fen}$ to be 30 % accurate. The measured NO mole fractions at 1.5 cm and $X_{NO,\ Fen}$ agree to within experimental error for Flames F2 and F3, which suggests that the observed shift in CH profile does not affect the NO formation significantly.

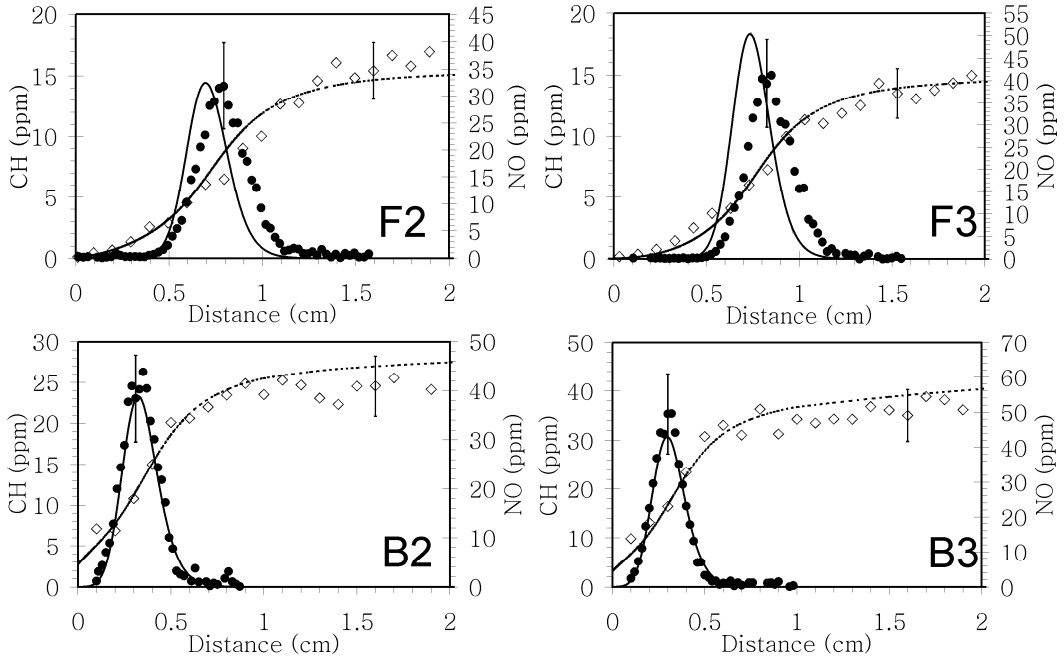

Figure 5.2 Measured and calculated CH and NO mole fractions without FGR (B2 and B3) and with FGR (F2 and F3). Points denote measurements: filled circles CH and open diamonds, NO. Lines denote calculated results: solid lines are CH and dashed lines are NO.

For comparison, the calculated and measured profiles of the CH and NO mole fractions for flames without FGR, but at the same mass flux as Flames F2 and F3, i.e., Flames B2 and B3 presented in Chapter 4, are also shown in Figure 5.2. The maximum CH mole fractions for both 4 and 5 slpm are roughly 50% lower when FGR is applied. As discussed in Chapter 4, assuming that all other variables in equation (1.11) do not change, we expect the same reduction in NO mole fraction as that for CH (i.e., ~50%). However, this is not the case, and the measured NO mole fractions for flames with FGR are on the average 25% lower. It is interesting to note that, although the maximum flame temperatures are significantly different (see Table 5.1), the temperatures at the peak of the CH mole fraction (see Figure 5.1) for flames with and without FGR differ only slightly (26 K and 40 K for 4 slpm and 5 slpm, respectively, well within the uncertainty of the measurements). This small change in temperature results in a negligible (<2%) change in $k_{f4}(T)/T$. Other factors such as mass flux increases marginally (<3%) as a consequence of FGR, and the CHEMKIN calculations also show a small increase (~8%) in the mean molecular weight $(\overline{W})$. The analysis indicates that the main contribution to the change in NO formation besides the reduction in the peak CH mole fraction is the

increase in the N_2 mole fraction. Due to the dilution of the cold gas mixture, the N_2 mole fraction changes from 0.43 (without FGR) to 0.60 (with FGR), corresponding to an increase of 28%. When considering all contributing factors, it is clear that the 50% decrease in CH mole fraction is compensated substantially by the increase (28%) of N_2 concentration in the cold gas mixture as a consequence of applying FGR.

5.5 Comparison between FGR and burner stabilization

In the previous studies of the influence of burner stabilization on NO formation [2,9,10] a strong correlation of Fenimore NO formation was observed with flame temperature. Therefore, it would be interesting to compare both methods of NO reduction at the same flame temperature. Towards this end, we compare Flames F2 and B1, having approximately the same flame temperature (see Table 5.1). Figure 5.3 shows the temperature profiles, approximated by equation (3.19), and the measured OH profiles for Flames B1 and F2. We note that the maximum temperature (T_{max}, Table 5.1) and maximum OH mole fraction of Flame F2 are, within the uncertainty of the measurements, in agreement with the profiles of Flame B1.

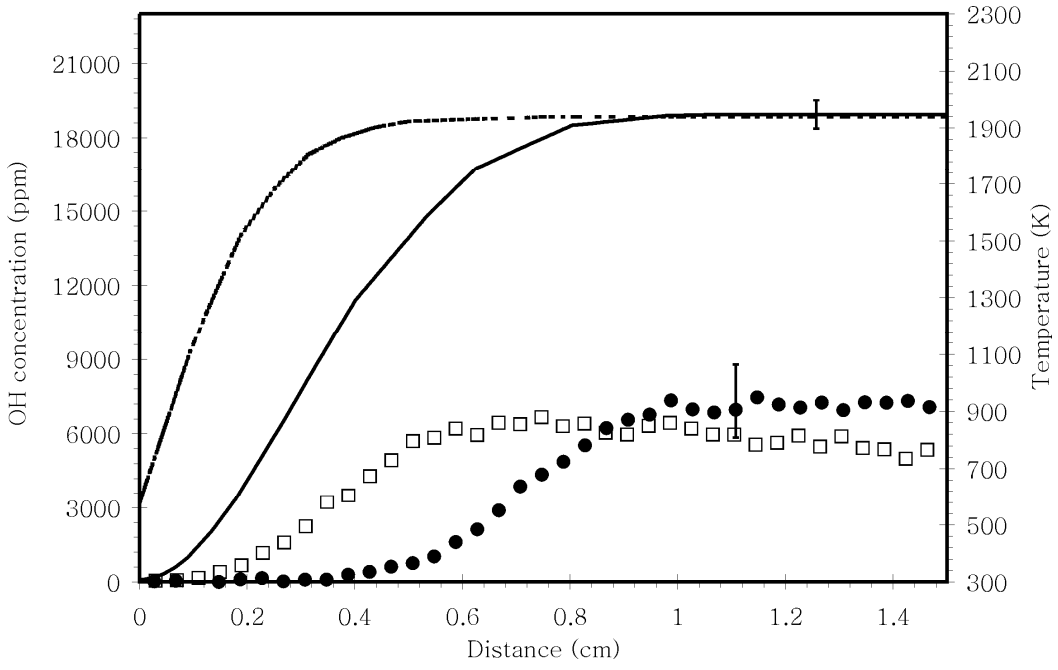

Figure 5.3 Fitted temperature and OH profiles for Flames B1 and F2. Lines denote temperature measurements: dotted line is Flame B1 and solid is Flame F2. Points denote OH mole fractions: squares denote Flame B1 and circles, Flame F2.

The measured CH and NO mole fractions in Flames B1 and F2 are shown in Figure 5.4, where the profiles for Flame F2 are shifted until the peaks of the CH profiles coincide. As can be seen in the figure, the measured CH and NO mole fractions for Flame F2 are very close to those measured in Flame B1. In other words, within the experimental uncertainty of the current measurements, at fixed flame temperature the NO emissions obtained by applying burner stabilization and FGR are identical.

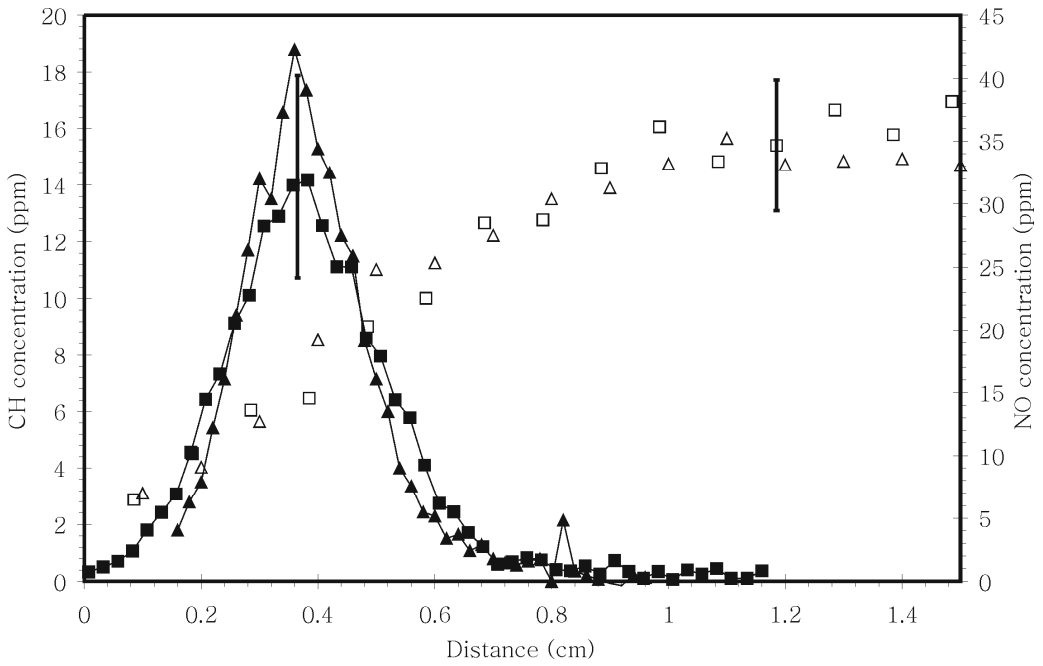

Figure 5.4 Measured CH and NO mole fractions for Flames B1 and F2. Triangles denote Flame B1 and squares denote Flame F2: open, NO and closed connected with line, CH.

.

5.6 Comparison between 'wet' and dry FGR

So far, we have considered the situation in which water has been removed from the flue gases. The good agreement between calculated and measured profiles for 35 Torr ϕ=1.3 premixed $CH_4/O_2/N_2$ flames with 'dry' FGR favors performing a numerical study of the effect on NO when water is also recycled back to the burner ('wet' FGR). Towards this end, the CHEMKIN calculations are also performed for the unburned fuel/oxidizer mixture containing water and carbon dioxide at γ=3. The CO_2/H_2O ratio is chosen such that it corresponds to that of flue gases in a stoichiometric methane/"air" (40% O_2) flame. Figure 5.5

shows the results of the calculations for the two premixed flames (wet and dry FGR), having the compositions $CH_4(14\%)/O_2(22\%)/N_2(53\%)/CO_2(3\%)/H_2O(8\%)$ or $CH_4(14\%)/O_2(22\%)/N_2(61\%)/CO_2(4\%)$. In both calculations the flow rate is kept at 4 slpm.

According to the calculations, the recycling of water has no significant effect on temperature and OH mole fractions. Further, the CH profiles are almost identical, but a significant decrease is observed in NO mole fractions (~18% at 1.5 cm).

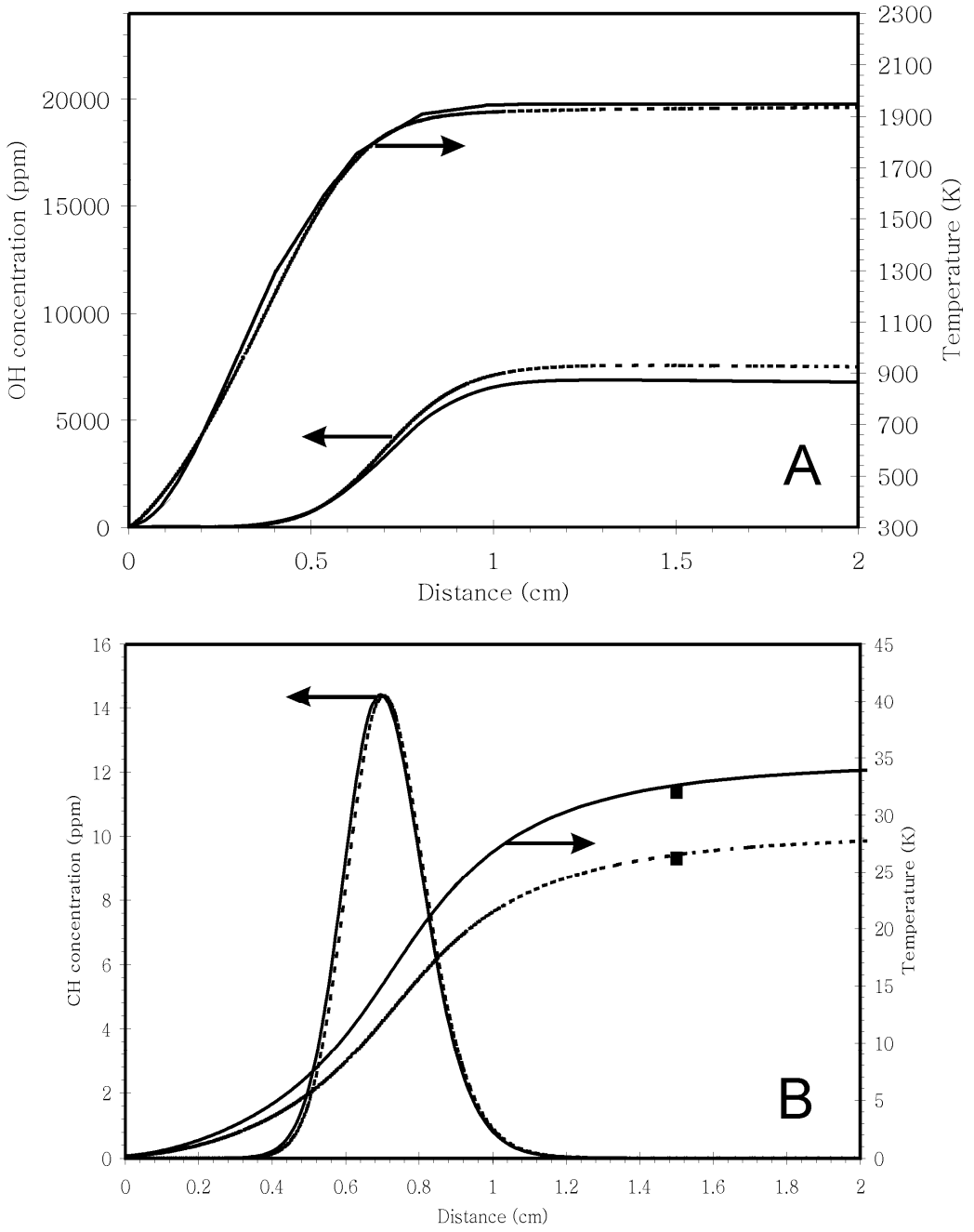

Figure 5.5. A) calculated temperature and OH profiles and B) calculated CH and NO profiles for 4 slpm 35 Torr ϕ=1.3 premixed CH_4/O_2(40%)/N_2(60%) flame when FGR is applied (γ=3). Solid lines denote results without water recycling and dotted lines denote calculations including water recycling. Profiles are calculated based on solving the energy equation Filled squares denote calculated amount of Fenimore NO (see text for details).

To provide insight into the origins of this substantial difference in NO formation, we estimate again the amount of Fenimore NO ($X_{NO,Fen}$) formed in these flames using equation (1.11). The integration was performed up to 1.5 cm in the calculated profiles.

As shown in Figure 5.5, the values of $X_{NO,Fen}$ show excellent agreement with calculated NO mole fractions. Since this comparison is based upon the CHEMKIN calculations, which have no experimental uncertainty, and all the NO arises from the Fenimore mechanism, we may analyze the various contributions to equation (1.11) more quantitatively than if this were experimental data. The effect of ρv on Fenimore NO can be neglected since the profiles shown in Figure 5.5 are calculated at constant mass flux. Based on Figure 5.5B we would expect that the influence of CH and temperature on Fenimore NO formation should be small, since water recycling shows almost no changes in the calculated profiles. And indeed, if we calculate the effect of these two parameters on $X_{NO,Fen}$ for the 'dry' FGR case, while using the CH or temperature profiles from the 'wet' FGR case, only a small reduction in $X_{NO,Fen}$ is found (0.2% for CH and 1.6% for temperature). In a similar fashion, the influence of the mean molecular weight ($\overline{W}$) is calculated, where small changes as a consequence of water recycling results in a 4% decrease in $X_{NO,Fen}$. In the discussion of 'dry' FGR, above, it was noted that the increase in the in-flame nitrogen mole fraction, caused by the dilution of the cold gas mixture, is an important factor for Fenimore NO formation, and can increase NO formation. When considering 'wet' FGR, the cold gas N_2 mole fraction decreases by 12% when water is recycled, which also decreases $X_{NO,Fen}$ by ~12%. When taking into account all the contributing factors, the total reduction in NO mole fraction corresponds exceedingly well with the calculated 18% decrease in NO concentration. However, from this discussion it is clear that the reduction of the N_2 mole fraction is the main contributor to the decrease in NO concentration when 'wet' FGR is applied.

5.7 Consequences for practical systems

Many practical systems, from household appliances to large-scale industrial burners, operate at least partially under fuel-rich conditions. As a rule, the fuel-rich flame gases in practical systems are ultimately mixed with air to oxidize residual H_2 and CO, both to reduce pollutant emissions and to

recover the enthalpy in these intermediate combustion products. Whereas burner stabilization and FGR are certainly useful for controlling the NO formed by the Zeldovich mechanism in the stoichiometric and lean regions of these flames, it was assumed [9] that "freezing out" the Zeldovich formation by reducing the flame temperature would leave a residual Fenimore contribution which, if unaltered by the control methods, would form a lower limit to the NO_x emissions. The previous studies at atmospheric pressure [2,9,10] suggested that burner stabilization and FGR could also result in a significant reduction in NO_x emissions from fuel-rich flames. In this thesis, for equivalence ratios ranging from 1.3 to 1.5, we observed in Chapter 4 a decrease in NO by ~40% with a temperature change of 230 K when decreasing the cold gas velocities by 5/3. Using FGR, we also observe a decrease of 20-30% for γ=3. These variations in NO formation were further seen clearly to be derived mechanistically from the observed changes in flame structure: specifically the changes in local temperatures, CH and N_2 mole fractions and residence times. The variation in NO formation reported here are consistent with those observed in the work at atmospheric pressure (see also Chapter 6, below). We therefore expect such reductions to be realizable in practice.

There are however other factors to be considered. An important characteristic for burners is the maximum thermal input [2]. For burner stabilization as a control strategy (radiant burners) it will be clear that a reduction in thermal input below the free flame burning velocity is essential for lowering the NO emissions; the maximum input is often limited to only a few hundred kilowatts per square meter. To increase the heat input, a larger burner surface is necessary, which is not always practicable. On the other hand, it was observed [2] that, although FGR also reduces the burning velocity, and thus in the 1-D approximation the maximum thermal input, the use of FGR is not limited to flat flames. Therefore, in principle FGR may have a significant advantage over burner stabilization. On the other hand, a practical drawback is that FGR complicates the operation of the burner system, since additional duct work must be laid to recirculate the flue gases to the burner head, and an adequate control system to regulate the amount of flue gases must be installed.

We further point out here that, although we observe significant reductions in NO mole fraction in fuel-rich premixed flames upon application of NO_x control strategies, we have not reached the low levels of NO_x, to single digits, possible using stoichiometric- or lean-premixed radiant burners [2,11]. In this

regard, perhaps the Fenimore contribution, albeit sensitive to control strategies, does indeed form a lower limit to NO formation; this being in the range of tens of ppm under the conditions studied in this thesis (Tables 4.1 and 5.1). Although this observation seems to discourage use of fuel-rich combustion for ultra-low emissions, there is a potential region in which rich premixing could be advantageous for NO_x control, i.e., preheated combustion. As observed at atmospheric pressure [10], the Zeldovich mechanism in preheated combustion leads to copious NO formation in oxygen-rich flames, while the Fenimore mechanism appears much less susceptible to preheating. Provided the "burnout" of the hot CO and H_2, referred to above, is done after substantial heat transfer, for example by using radiant burners, this method could lead to significantly lower NO_x emissions. However, as suggested in Chapter 4 (and references [2,9,10]), at very rich equivalence ratios the lower flame temperatures caused by the NO_x control strategy could result in residual fixed nitrogen species, which will form NO upon burnout. A recommendation from this study is to extend the measurements performed here to fuel-rich preheated mixtures.

Lastly, we point out that our studies indicated that calculations using GRI-Mech 3.0 chemical mechanism predicts the trend in NO mole fractions very well for the flames studied, in spite of possible mechanistic shortcomings. For the flames at ϕ=1.3, the predicted NO mole fractions even showed quantitative agreement with the measurements. Therefore, we could recommend GRI-Mech 3.0 for calculating the trends in NO formation with burner stabilization or FGR. Of course, care must be taken when the mechanism is being used outside the area in which it has been compared with experiments.

5.8 Conclusions

In this study, we applied 'dry' FGR on 35 Torr ϕ=1.3 premixed methane/oxygen/nitrogen flames at flow rates of 4 and 5 slpm. The consequence of applying FGR for both flames is a decrease of ~50% for the maximum CH mole fraction and a decrease of ~25% in the NO mole fraction. Detailed calculations using GRI-Mech 3.0 predict the results for the flames studied quantitatively, but predict CH profiles closer (~0.1 cm) to the burner surface. However, calculations of the amount of Fenimore NO, using the measured CH and temperature profiles, showed that the observed shift has no

effect on the analysis of the NO formation in these flames. The increase in the mole fraction of molecular nitrogen in the flame, caused by the dilution of cold gas mixture as a consequence of applying FGR, substantially compensates the decrease in peak CH mole fraction and is primarily responsible for the reduction in NO being significantly lower than expected from the change in CH mole fraction. A comparison of FGR and burner stabilization (at fixed flame temperature) showed no difference in measured OH, CH and NO mole fractions for 35 Torr ϕ=1.3 premixed methane/oxygen/nitrogen flames. Calculations using GRI Mech 3.0 indicate that when water is also recycled, thus reducing the molecular nitrogen concentration in the cold gas mixture, a larger decrease in NO can be expected.

Bibliography

1. Muzio, L. J. and Quartucy, G. C., "Implementing NOx Control: Research to Application", *Prog.Energy Combust.Sci.* **23**, 233-266 (1997)

2. Mokhov, A. V. and Levinsky, H. B., "*A LIF and CARS Investigation of Upstream Heat Loss and Flue-Gas Recirculation As NOx Control Strategies for Laminar, Premixed Natural-Gas/Air Flames*", 28th Symp. (Int.) Combust., 2467-2474 (2000)

3. Smith, G. P., Golden, D. M., Frenklach, M., Moriarty, N. W., Eiteneer, B., Goldenberg, W., Bowman, C. T., Hanson, R., Gardiner, W. C, Lissianski, V., and Qin, Z., http://www.me.berkeley.edu/gri_mech/.

4. Berg, P. A., Smith, G. P., Jeffries, J. B., and Crosley, D. R., "*Nitric Oxide Formation and Reburn in Low-Pressure Methane Flames*", 27th Symp. (Int.) Combust., 1377-1383 (1998)

5. Berg, P. A., Hill, D. A., Noble, A. R., Smith, G. P., Jeffries, J. B., and Crosley, D. R., "Absolute CH Concentration Measurements in Low-Pressure Methane Flames: Comparisons With Model Results", *Combust.Flame* **121**, 223-235 (2000)

6. Heard, D. E., Jeffries, J. B., Smith, G. P., and Crosley, D. R., "Lif Measurements in Methane Air Flames of Radicals Important in Prompt-No Formation", *Combust.Flame* **88**, 137-148 (1992)

7. Pillier, L., El Bakali, A., Mercier, X., Rida, A., Pauwels, J. F., and Desgroux, P., "*Influence of C-2 and C-3 Compounds of Natural Gas on NO Formation: an Experimental Study Based on LIF/CRDS Coupling*", 30th Symp. (Int.) Combust., 1183-1191 (2005)

8. Kee, R. J., Rupley, F. M., and Miller, J. A., "CHEMKIN II: A Fortran Chemical Kinetics Package for the Analysis of Gas-Phase Chemical Kinetics", Report No.SAND89-8009, Sandia National Laboratories ,1989

9. Mokhov, A. V. and Levinsky, H. B., "*A LIF and CARS Study of the Effects of Upstream Heat Loss on NO Formation From Laminar*

Premixed Burner-Stabilized Natural-Gas/Air Flames", 26th Symp. (Int.) Combust., 2147-2154 (1996)

10. Sepman, A. V, Mokhov, A. V., and Levinsky, H. B., "A Laser-Induced Fluorescence and Coherent Anti-Stokes Raman Scattering Study of NO Formation in Preheated, Laminar, Rich Premixed, Methane/Air Flames", *Symp.(Int.) Combust.* **29**, 2187-2194 (2002)

11. Bouma, P. H. and De Goey, L. P. H., "Premixed Combustion on Ceramic Foam Burners", *Combust.Flame* **119**, 133-143 (1999)